*Conference Proceedings*

# Imaging via Cosmic Muon Induced Secondaries

**Gergő Hamar,[1] Kristina Demirhan,[2] Dániel Hajnal,[1] Dusan Mrdja,[2] Gábor Galgóczi,[1] and Dezső Varga[1]**

[1]*HUN-REN Wigner Research Centre for Physics, Budapest, Hungary*

[2]*University of Novi Sad, Faculty of Sciences, Department of Physics, Novi Sad, Serbia*

*Corresponding author: Gergő Hamar*
*Email address: hamar.gergo@wigner.mta.hu*

## Abstract

As cosmic muons traverse a target, they interact with it, producing secondary radiation, whose spectrum depends on the material-composition of the target. This imaging technique is sensitive to low-Z materials as well, opening a novel noninvasive material-identification method for medium-sized obscure targets. Our Hungarian-Serbian collaboration pioneered in demonstrating experimentally this unique method, using gaseous trackers for the muons and a scintillator array and germanium detector for the secondaries. Results have proven imaging possibilities ranging from metals to soft-tissue targets. Corresponding Geant4 simulations have revealed forward-sideward asymmetry and sensitivity to the electron/gamma ratio. The former is materialized in a new experimental setup, with large coverage via segmented scintillator arrays, and a combined and compact DAQ, with an electron-tagging possibility. The paper describes the recent results in imaging via secondaries and details the new enhanced experimental setup and its first results.

*Keywords:* muography, material identification, gaseous detectors
*DOI:* 10.31526/JAIS.2024.494

## 1. INTRODUCTION

Muography is a novel field where particle physics instrumentation-based experiments are used to detect cosmic muons to investigate the internal structure of large objects, founding a new survey method usable in geophysics, geology, archaeology, and industry.

The most common and known type is absorption muography, where lower energy muons get absorbed in the object; the integrated density-length along the path of the crossing muon is correlated with the decrease in the flux map, thus producing radiographic density-images of large objects [1]. Both surface-based and underground experiments are of interest and are able to study, e.g., volcanoes [2], pyramids [3] caves [4], mines [5], or any kind of larger-scale density-anomalies.

Muon scattering tomography uses internal multiple scattering, making it highly sensitive to high-Z nuclei. In this case, the direction of the incoming and outgoing muon is tracked; thus, the scattering regions can be located in space [6]. The main applications could be in industrial scanners or national security [7].

However, there is a third type of interaction that takes place: as muons interact with a target secondary particle emission can occur [8] (mostly from bremsstrahlung, delta rays, and their secondary interactions). The spectra of these secondaries depend on the material composition and the shape of the target; thus, their measurement could lead to a novel technique for nondestructive material identification for low-Z materials as well. As the penetrating muons create secondaries well inside the target, the composition of deeper layers could be revealed (unlike surface-sensitive methods).

The first experimental system detecting secondary gammas with muon tracking was developed by our Serbian-Hungarian collaboration [9]. Although a few purely simulation works have been done in this direction [10, 11], proper experimental measurements are required for validation or tuning of the simulation parameters making the limitation of the technology clear.

## 2. THE MUCA EXPERIMENT

The MUCA (Muon Camera) Experiment was pioneering for imaging with cosmic muon-induced secondary particles [9]. In its recent version, the target is placed into a 50 cm-sided cube, surrounded by 5 cm thick plastic scintillators on the four sides to efficiently detect the secondary gamma and electron radiation (typically their energy the between 100 keV and few MeV). Above the target volume, the incoming muons traverse a multilayered gaseous tracker, similar to the one designed for muography measurements by the WignerRCP group [4].

Since first measurements, proof-of-concept imaging, and qualitative identification of various targets have already been shown [9], we focus now on a quantitative analysis from the data of the MUCA experiment.

As MUCA captures only the sideward leaving secondary particles (see Figure 2 (left)), thus the vertical position of the Target inside the target volume defines its acceptance. Moving the Target upwards, the geometric acceptance decreases, while one starts

to capture more from the forward-leaving secondaries. Let us define the "yield" as the ratio of detected secondary electrons and gammas produced within the target, with respect to the number of the traversing muons.

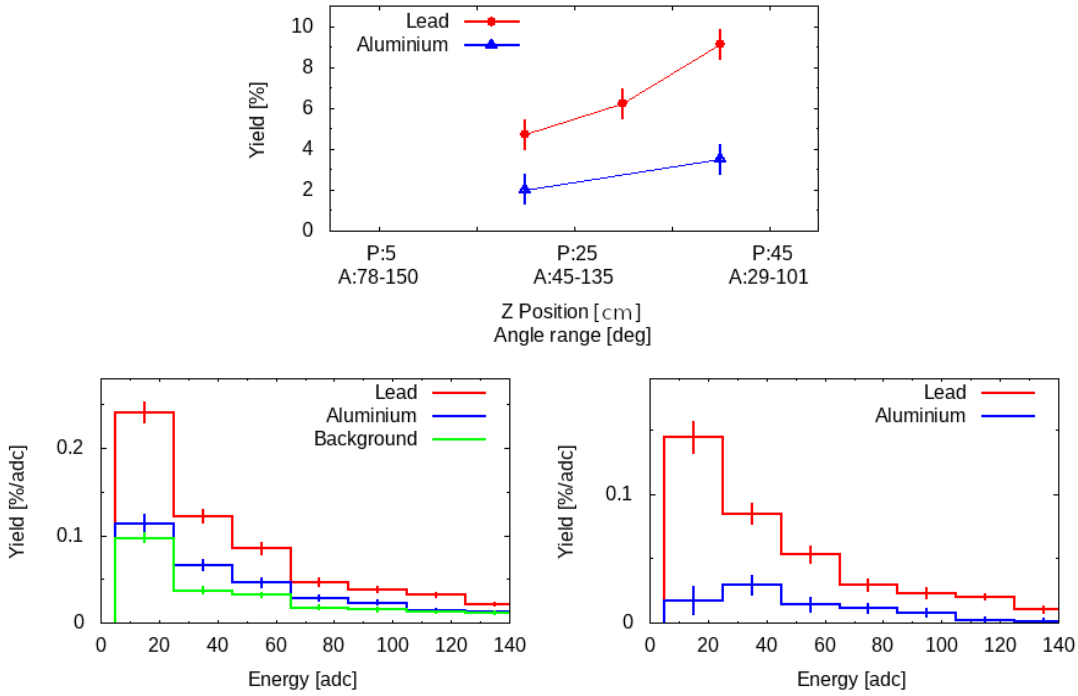


FIGURE 1: Yield of secondaries in MUCA for aluminum and lead targets. *Top*: height scan shows an increase in yield toward the forward direction. *Left*: raw detected spectra for the targets and an empty one (green). *Right*: background-subtracted spectra show clear differences in Al and Pb targets.

Geant4 simulations predict an increase in the yield for more forward configurations [12]; thus, a simple measurement series was done with targets in various vertical positions. Let us mark $Z = 0$ as the bottom of the target volume (thus $Z = 25\,\text{cm}$ is the middle); the acceptance can be demonstrated with the angle range and the scintillators are seen from the target (lower edge, higher edge). Figure 1 (top) shows an increase in the yield for more forward-like configurations, experimentally confirming the expectation.

As the spectra of the secondaries depend on the target material, that could later be used for material identification. Figure 1 (left) shows the measured spectra for aluminum, lead, and empty-target configurations (at $Z = 40\,\text{cm}$). The background-subtracted spectra in Figure 1 (right) verify that not only the yield but also the shape of the spectrum is sensitive to the material type.

## 3. UPGRADE: THE COMIS EXPERIMENT

Based on the proven good performance, practical issues of operation, and simulation predictions, we have decided to design a new experimental setup taking into account the following for the upgrade:

(i) *Forward region*: Measurement results (above) and simulation studies [12] both proved that the forward region covers a large ratio of secondaries; thus, that shall be covered with scintillators as well.

(ii) *Multichannel readout*: When the muon passes a forward scintillator, the deposited energy (order of 10 MeV) is way higher than for the secondaries. Thus, the segmentation of the forward scintillator is required, together with the separate readout of all the items (to exclude the muon).

(iii) *Electron/Gamma tagging*: Simulations predict that the electron/gamma ratio highly depends on the material type; thus, an $e/\gamma$ tagger could enhance the identification capability.

(iv) *Combined DAQ*: The former items require a new data acquisition system, with tracking modules and multichanneled analog-digital converters (ADCs), preferably with a compact and portable design.

Figure 2 shows a sketch of the mentioned upgrades, on its left side is the MUCA setup, and on its right side is the planned upgraded experiment.

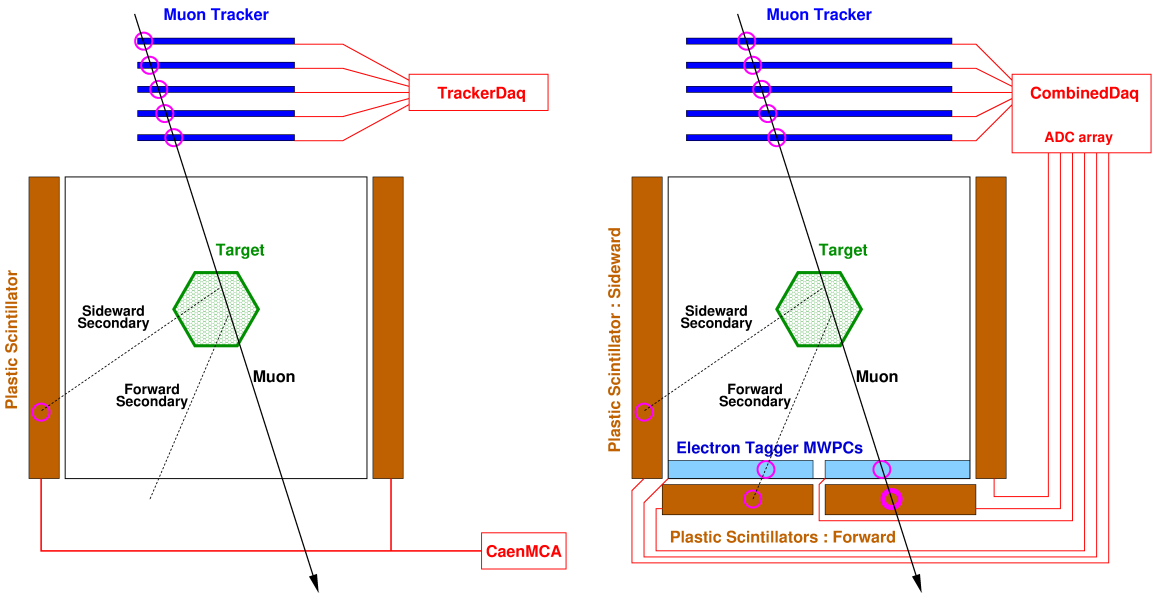


FIGURE 2: Schematic side-view drawing of the recent and upgraded experiment setup. MUCA includes sideward scintillators connected together to a CAEN multichannel-analyzer and a fully separate system for the trackers. The upgrade includes segmented forward scintillators, electron-tagging chambers, and a combined data acquisition system.

The design has been finalized and the new experiment has been implemented; thus, the COsmic Muon Induced Secondaries (COMIS) experiment has been established. The target volume remains about 50 cm cubed, surrounded by four pieces of $50 \times 50 \times 5\,\mathrm{cm}^3$ plastic scintillators (EPS100), while the forward region by four similar $25 \times 25 \times 5\,\mathrm{cm}^3$ ones.

The tracking station uses five layers of large-area ($51 \times 51\,\mathrm{cm}^2$) Close Cathode Chambers [13, 14] with 2 mm spatial resolution and >98% efficiency to ensure the precise tracking of the muon. (Due to mechanical issues, the tracker has been placed underneath the target volume, as can be seen in Figure 3.)

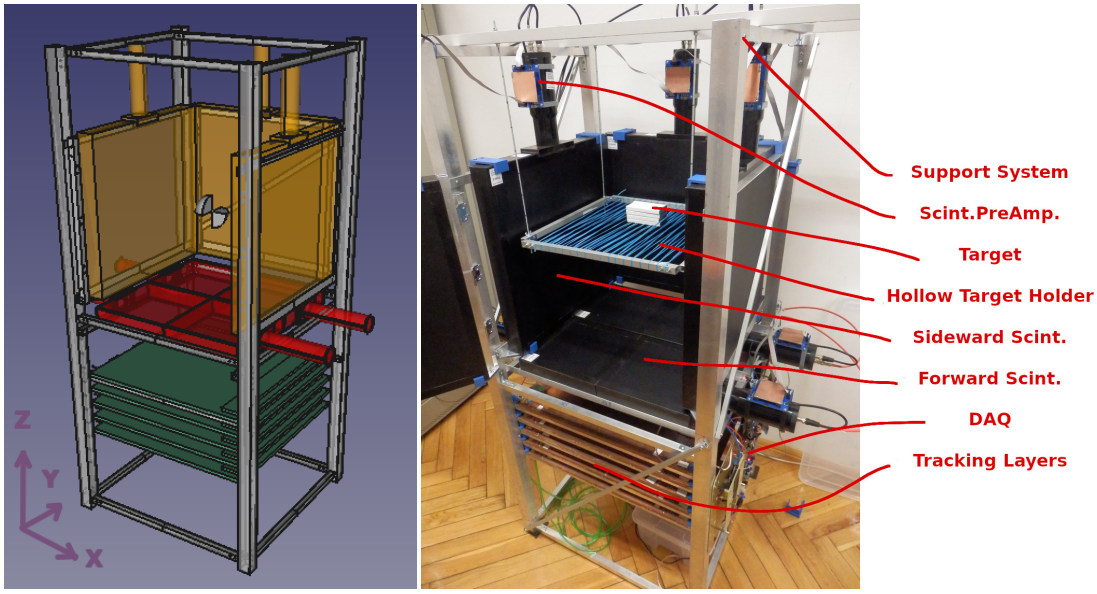


FIGURE 3: Drawings and photos of the COMIS experiment (with its door opened) in Budapest.

The $e/\gamma$ tagging will be done via thin-cathode gaseous multiwire chambers (MWPCs), where charged particles will leave a signal, while photons in the expected energy range have a very small probability of interaction. This tagger will be built for the forward part, with the same segmentation as the scintillators (for the same reason, to exclude the muon).

Figure 3 (left) shows the CAD drawings, while Figure 3 (right) shows a photo of the COMIS experiment.

The combined data acquisition is driven by a RaspberryPi microcomputer and uses similar boards and features as the Regard Muograph detectors [15], so the readout scheme of the tracking layers is as cited above. Each scintillator has a preamplifier, with a high-resolution ADC for small signals (secondaries) and a trigger output for higher signals (crossing muon). The trigger output of the forward scintillators is used to trigger the readout system, while events are recorded if the tracking layers also have hits. A close-up photo of the DAQ and the lower part of the COMIS can be seen in Figure 4.

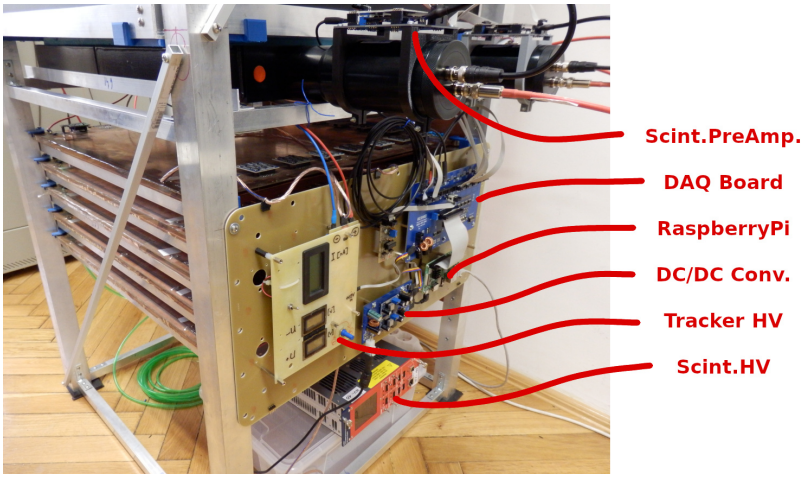


FIGURE 4: Photo of the data acquisition system of the COMIS experiment.

## 4. FIRST RESULTS

Operational validation of the COMIS experiment has been done via imaging of a simple target (thin lead piece, shown above in Figure 3 (right)). The imaging procedure first reconstructs the muon trajectory from the tracker data, gets its intersection point with the plane of the target, and assigns the event to the corresponding point/pixel. Secondary particle hits are accepted for each scintillator if the muon-triggered readout amplitude is above their given threshold. The *yield* (as a probability of having a detected secondary for a muon) thus can be defined for each pixel, resulting in a yield map for each scintillator. As MUCA uses about a day for exposure, this study used the same. Using the feature of the separate signal handling of the scintillators, one can get separate yield measurements from each one, leading to $4+4$ yield maps.

For this study, we have used the sideward scintillators, named according to their position ($X/Y$ and $+/-$) with respect to the target volume (the coordinate system was defined in Figure 3 (left)).

The background has been calculated by having a measurement without any target inside; thus, it contains the electrical noise and the occasional secondaries coming from the mechanical structure of the experiment itself. The verification of the experiment was done via imaging a simple lead target ($10 \times 5 \times 4\,\mathrm{cm}^3$ brick) shown in Figure 3 (right). The measured two-dimensional yield maps (after background subtraction) are shown in Figure 5 (left) with a color scale for the eye (ranging from 0 to 3%). The lead target is clearly visible on all of them. For quantitative investigation, slices of the yield maps are shown in Figure 5 (right): 3-3 slices for scintillators "$X+$" and "$X-$" (direction of slices are marked in Figure 5 (left) with red lines), and the same slices for the background (targetless) run as well.

The integrated yield is consistent with the previous measurements of the MUCA setup. However, the measured yield of secondaries in Figure 5 (left) and (right) shows a clear nonuniform/nonconstant behavior. Each scintillator sees an image with a higher yield closest to them and a decreasing tendency toward the other side of the target, reasoned as the effect of internal absorption of the secondaries within the target. This type of information could later be used in the foreseen identification process as well.

## 5. SUMMARY AND OUTLOOK

The pioneering work of experimental implementation of imaging via the detection of COMIS has been carried on. We have experimentally proven that different materials could have different measured spectra, which would be essential for later identification applications. The simulation expectations of a higher-yield forward region have been qualitatively verified.

A new and upgraded setup, the COsmic Muon Induced Secondaries experiment (COMIS), has been designed and constructed, with forward coverage, multisignal handling, and compact DAQ. The first results have proven its operational validity.

While the commissioning is still ongoing, calibration-based unification and fine-tuning will be performed, the $e/\gamma$ tagger will be constructed, and then a detailed scan of various material types is foreseen, measuring the detectable spectra and correlating with simulations.

This could establish the basis of this uncommon nondestructive material-identification method.

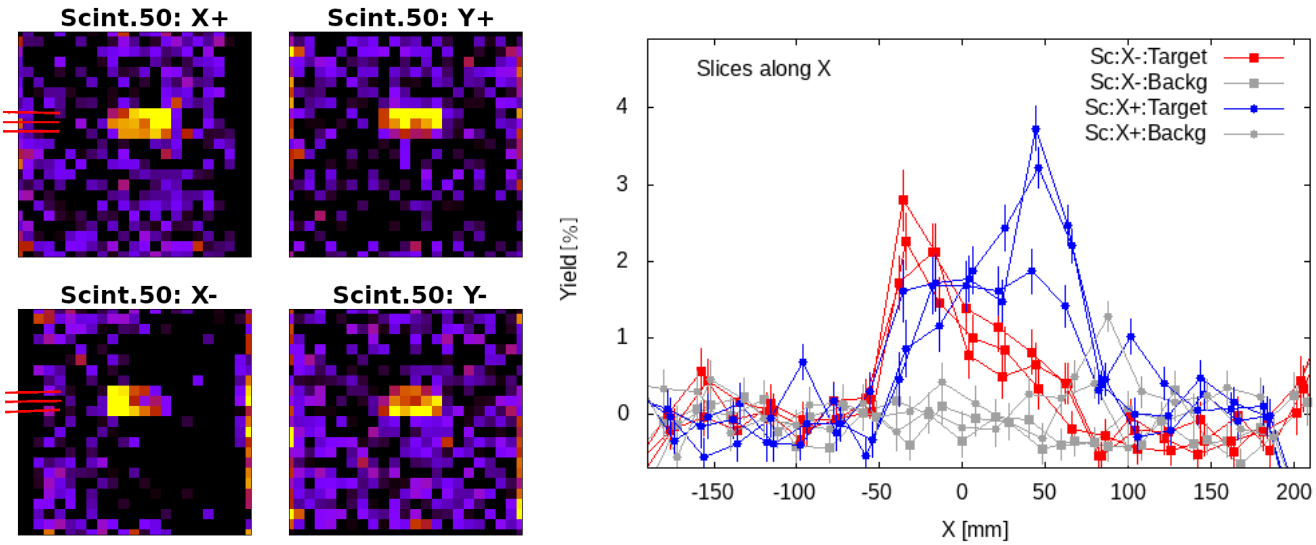


FIGURE 5: First images of a thin lead brick by the COMIS using the four scintillators aside. *Left*: 2D yield images with color scale "for the eye". Red lines indicate the direction and position of slices for the next figure. *Right*: 1D slices of the yield maps for two scintillators, with and without the target.

## CONFLICTS OF INTEREST

The authors declare that there are no conflicts of interest regarding the publication of this paper.

## ACKNOWLEDGMENTS

The authors gratefully acknowledge the financial support of the Hungarian OKTA-FK-135349, ELKH-KT-SA-88/2021, TKP2021-NTKA10, TÉT-2021-00223, and the János Bolyai Scholarship of the HAS, and support of the Ministry of Science Technological Development and Innovation of the Republic of Serbia with Grant No. 451-03-47/2023-01/200125.

## References

[1] N. Lesparre et al., *Geophysical muon imaging: feasibility and limits*, Geophys. J. Int. **183**, 1348 (2010).
[2] L. Oláh et al., *High-definition and low-noise muography of the Sakurajima volcano with gaseous tracking detectors*, Sci. Rep. **8**, 3207 (2018).
[3] K. Morishima et al., *Discovery of a big void in Khufu's Pyramid by observation of cosmic-ray muons*, Nature **552**, 386 (2017).
[4] L. Oláh et al., *CCC-based Muon Telescope for Examination of Natural Caves*, Geosci. Instrum. Method. Data Syst. **1**, 229 (2012).
[5] D. Schouten, *Muon geotomography: selected case studies*, Philos. Trans. R. Soc. **A 377**, 2137 (2018).
[6] S. Pesente et al., *First results on material identification and imaging with a large-volume muon tomography prototype*, Nucl.Instrum.Meth. **A 604**, 738 (2009).
[7] K. Borozdin et al. *Radiographic imaging with cosmic-ray muons*, Nature **422**, 277 (2003).
[8] K. Bikit et al., *Investigation of cosmic-ray muon induced processes by the MIREDO facility*, Applied Radiation and Isotopes **87**, 77 (2014).
[9] I. Bikit et al., *Novel approach to imaging by cosmic-ray muons*, Europhysics Letters **113** n.5, 58001 (2016).
[10] X. Ji et al., *A novel 4D resolution imaging method for low and medium atomic number objects at the centimeter scale by coincidence detection technique of cosmic-ray muon and its secondary particles*, Nucl. Sci. Tech **33**, 2 (2022).
[11] M. P. Prada et al., *Analysis of Secondary Particles as a Complement to Muon Scattering Measurements*, Instruments **2022** 604066 (2022).
[12] G. Galgóczi et al., *Imaging by muons and their induced secondary particles—a novel technique*, J. Instr. **15** , C06014 (2020).
[13] D. Varga, G. Hamar, and G. Kiss, *Asymmetric multi-wire proportional chamber with reduced requirements to mechanical precision*, Nucl.Instrum.Meth. **A 648**, 163 (2011).
[14] D. Varga, G. Hamar, G. Bencédi, and G.Kiss, *Close Cathode Chamber: Low material budget MWPC*, Nucl.Instrum.Meth. **A 698**, 11 (2013).
[15] D. Varga et al., *Construction and Readout Systems for Gaseous Muography Detectors*, J. Adv. Instrum. in Science **2022** 307 (2022).